



OPEN

SUBJECT AREAS:

ORGANIC LEDs
CHEMICAL ENGINEERINGReceived
1 April 2014Accepted
24 July 2014Published
14 August 2014Correspondence and
requests for materials
should be addressed to
J.Y.L. (leej17@
dankook.ac.kr)

Above 20% external quantum efficiency in novel hybrid white organic light-emitting diodes having green thermally activated delayed fluorescent emitter

Bo Seong Kim, Kyoung Soo Yook & Jun Yeob Lee

Department of Polymer Science and Engineering, Dankook University 126, Jukjeon-dong, Suji-gu, Yongin, Gyeonggi, 448-701, Korea.

High efficiency hybrid type white organic light-emitting diodes (WOLEDs) combining a green thermally activated delayed fluorescent (TADF) emitting material with red/blue phosphorescent emitting materials were developed by manipulating the device architecture of WOLEDs. Energy transfer between a blue phosphorescent emitting material and a green TADF emitter was efficient and could be managed by controlling the doping concentration of emitters. A high quantum efficiency above 20% was achieved in the hybrid WOLEDs by optimizing the device structure of the hybrid type WOLEDs for the first time and the device performances of the hybrid WOLEDs were comparable to those of all phosphorescent WOLEDs.

White organic light-emitting diodes (WOLEDs) have been developed for application in display and lighting devices^{1–3}, and one of critical issues of WOLEDs is power efficiency which is determined by driving voltage and external quantum efficiency. In order to improve the power efficiency of WOLEDs, the driving voltage of the WOLEDs should be reduced and the quantum efficiency should be improved. In particular, the quantum efficiency of the WOLEDs should be enhanced for high power efficiency.

There have been several approaches to increase the quantum efficiency of WOLEDs. The most effective way was to use phosphorescent emitting materials instead of fluorescent emitting materials as the emitter of WOLEDs^{1,4–11}. The quantum efficiency of WOLEDs could be improved above 20% using the phosphorescent emitters due to theoretically four times higher quantum efficiency of the phosphorescent emitters. Red, green and blue or yellow and blue triplet emitters were mixed in a single emitting layer or stacked in the multilayer structure to fabricate high efficiency WOLEDs. The other way was to combine a blue fluorescent emitter with red and green phosphorescent emitters^{2,12–15}. In general, blue fluorescent emitters are not compatible with red and green phosphorescent emitters due to triplet exciton quenching of phosphorescent emitters by the fluorescent blue emitters. However, the triplet exciton quenching of red and green phosphorescent emitting materials can be suppressed by adopting high triplet energy blue fluorescent emitting materials¹⁵. In this case, the singlet excitons of the blue emitting materials are used for blue emission, while the triplet excitons of the blue emitter are utilized for energy transfer to red and blue triplet emitters. Therefore, the combination of the blue fluorescent emitters with red/green phosphorescent emitters could produce high efficiency WOLEDs. However, it was difficult to develop high efficiency and high triplet energy blue fluorescent emitting materials and the efficiency of the hybrid type WOLEDs was rather limited.

Recently, thermally activated delayed fluorescence (TADF) emitting materials were developed as high efficiency fluorescent emitting materials^{16–27}. The TADF emitters could show close to 100% internal quantum efficiency because both singlet and triplet excitons can be harvested for light emission¹⁶. Therefore, the TADF emitters can be effectively adopted as the emitters for WOLEDs because they may not quench triplet excitons of the phosphorescent emitters.

In this work, high efficiency hybrid WOLEDs were developed using green TADF emitter and red/blue phosphorescent emitters. A two emitting layer stack structure was used to fabricate the hybrid WOLEDs.



Energy transfer between phosphorescent and TADF emitters was observed and high quantum efficiency of 20.2% was demonstrated using the hybrid WOLEDs. This work is the first demonstration of above 20% external quantum efficiency in hybrid WOLEDs. In particular, high quantum efficiency was achieved in the hybrid WOLEDs with the green fluorescent emitter for the first time.

Results

Device performances of the hybrid green and blue devices. In general, the triplet excitons of fluorescent emitters cannot be utilized for light emission because the transition from triplet excited state to singlet ground state is forbidden. However, TADF emitters can harvest the triplet excited state for light emission via reverse intersystem crossing due to small singlet and triplet energy difference¹⁶. Therefore, the TADF emitters may be compatible with phosphorescent emitters and may not quench triplet emission of phosphorescent emitters.

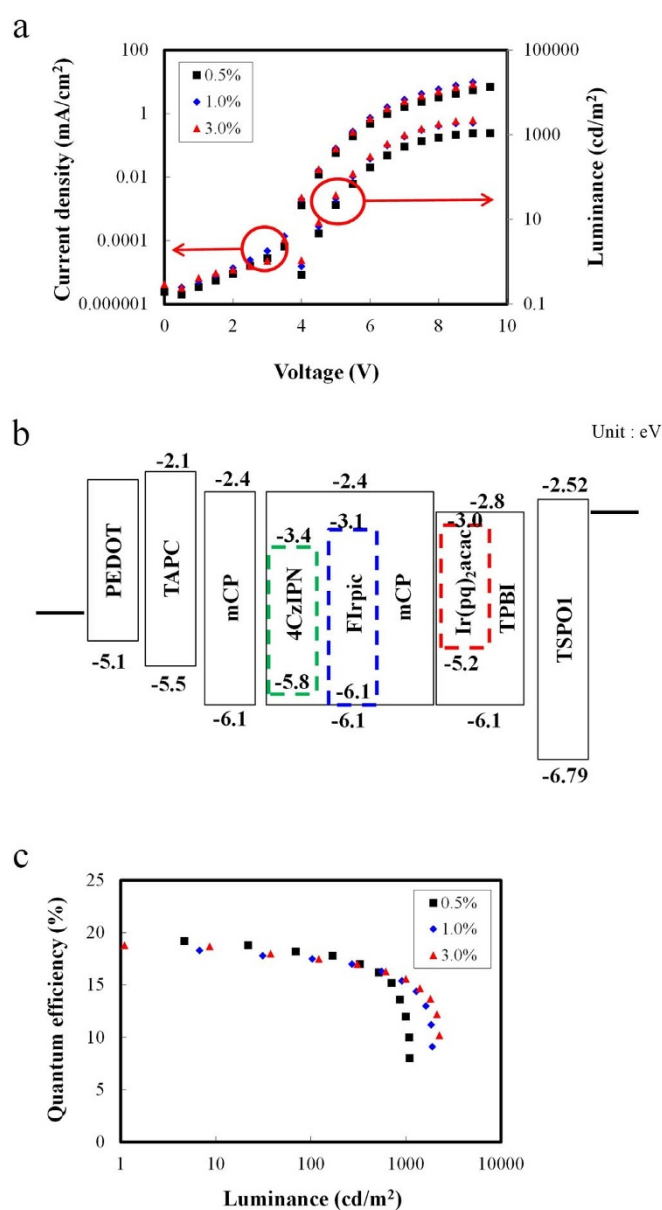


Figure 1 | Current density-voltage-luminance curves (a), energy level diagram (b) and quantum efficiency-luminance curves (c) of mCP:FIrpic:4CzIPN devices according to doping concentration of 4CzIPN. Doping concentration of FIrpic was 5%.

Hybrid organic light-emitting diodes (OLEDs) with blue emitting iridium(III) bis[(4,6-difluorophenyl)-pyridinato-N,C^{2'}]picolinate (FIrpic) and green emitting (4s,6s)-2,4,5,6-tetra(9H-carbazol-9-yl) isophthalonitrile (4CzIPN) were fabricated to explore the possibility of using the hybrid emitting layer in the hybrid WOLEDs. The FIrpic triplet emitter and 4CzIPN TADF emitter were doped in common N,N'-dicarbazoyl-3,5-benzene (mCP) host. Figure 1(a) shows current density-voltage-luminance curves of the hybrid OLEDs doped with FIrpic and 4CzIPN. Doping concentration of FIrpic was 5% and the doping concentrations of 4CzIPN were 0.5%, 1% and 3%. The current density and luminance of the hybrid OLEDs were low at 0.5% doping concentration because of electron trapping by 4CzIPN as shown in energy level diagram in Figure 1(b). As there was 1.0 eV LUMO level difference between mCP and 4CzIPN, electrons are easily trapped by 4CzIPN, resulting in reduced current density at 0.5% 4CzIPN doping concentration.

Quantum efficiency-luminance curves of the hybrid OLEDs according to doping concentration of 4CzIPN are presented in Figure 1(c). Maximum external quantum efficiency of the hybrid OLEDs was 19.2% at 0.5% doping concentration and above 18% external quantum efficiency was obtained at other doping concentrations. Considering that the quantum efficiency of mCP:FIrpic device is below 20%, the high quantum efficiency of the hybrid OLEDs indicates that the 4CzIPN does not quench the triplet emission of FIrpic. The triplet energy of FIrpic is transferred to 4CzIPN and contributes to TADF emission of 4CzIPN.

Electroluminescence (EL) spectra of the green/blue hybrid OLEDs are shown in Figure 2. The green emission of 4CzIPN was very weak at 0.5% doping concentration, but it was intensified at high doping concentration. At 3% 4CzIPN doping concentration, the blue emission of FIrpic appeared as a weak shoulder in spite of 5% doping concentration of FIrpic, implying energy transfer from FIrpic to 4CzIPN. There are three main energy transfer processes in mCP:FIrpic:4CzIPN hybrid OLEDs. Energy transfer processes from mCP to FIrpic, mCP to 4CzIPN and FIrpic to 4CzIPN dominate the blue and green emission of the hybrid OLEDs as will be shown in the PL spectra of the mCP:FIrpic:4CzIPN films. EL spectra of the mCP:FIrpic:4CzIPN devices were similar to PL spectra of the mCP:FIrpic:4CzIPN films with the same FIrpic and 4CzIPN doping concentrations.

Device performances of the hybrid white devices. Based on the device data of the mCP:FIrpic:4CzIPN hybrid OLEDs, WOLEDs

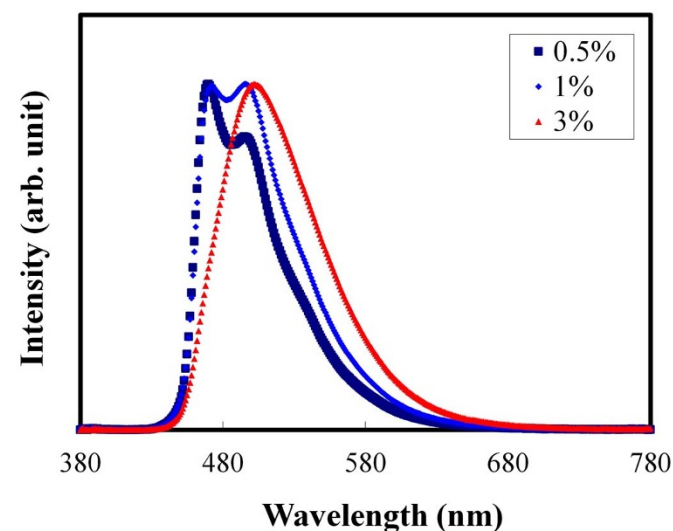


Figure 2 | EL spectra of mCP:FIrpic:4CzIPN devices according to the doping concentration of 4CzIPN. Doping concentration of FIrpic was 5%.



were fabricated by stacking the mCP:Firpic:4CzIPN emitting layer and TPBI:Ir(pq)₂acac emitting layer. The device structure of the WOLEDs was indium tin oxide (ITO, 50 nm)/poly(3,4-ethylenedioxythiophene):poly(styrenesulfonate) (PEDOT:PSS, 60 nm)/4,4'-(cyclohexane-1,1-diyl)bis(N-phenyl-N-p-tolylaniline) (TAPC, 20 nm)/mCP (10 nm)/mCP:Firpic:4CzIPN (12.5 nm)/TPBI:Ir(pq)₂acac (12.5 nm, 3%)/diphenylphosphine oxide-4-(triphenylsilyl)phenyl (TSPO1, 35 nm)/LiF (1 nm)/Al (200 nm). Doping concentrations of 4CzIPN was fixed at 1% and the doping concentrations of Firpic were 5% and 10% to control the emission zone of the WOLEDs. Figure 3(a) shows current density-voltage-luminance curves of the WOLEDs with different Firpic doping concentrations. The current density of the WOLEDs was increased at high Firpic doping concentration because of better charge hopping between Firpic dopants. However, the luminance was similar irrespective of Firpic doping concentration, which may be due to rather low recombination efficiency of the WOLEDs at 10% Firpic doping concentration.

Quantum efficiency-luminance curves of the WOLEDs are shown in Figure 3(b). High quantum efficiency was obtained at 5% Firpic doping concentration and maximum quantum efficiency of the hybrid WOLEDs was 20.2%, which was comparable to that of all phosphorescent WOLEDs. The quantum efficiency was slightly decreased at 10% Firpic doping concentration and maximum quantum efficiency of the hybrid WOLEDs was 18.5%.

EL spectra of the hybrid WOLEDs are presented in Figure 4. The hybrid WOLEDs exhibited relatively strong red emission compared to blue/green emission. The blue/green emission was intensified at 10% Firpic doping concentration because of recombination zone

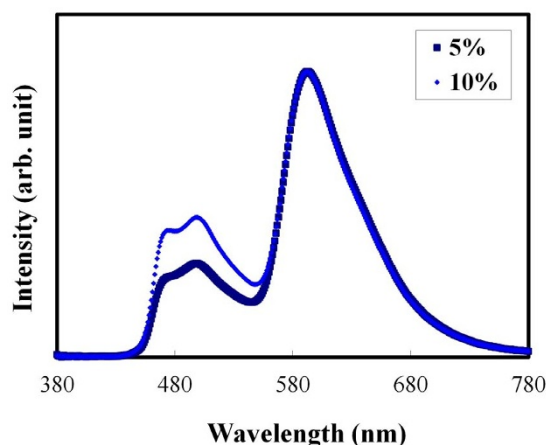


Figure 4 | EL spectra of the hybrid WOLEDs with different Firpic doping concentrations.

shift from the red emitting layer to the blue/green emitting layer by better electron hopping through Firpic dopants. However, the recombination zone was mostly distributed over the red emitting layer considering the strong red emission of the WOLEDs. Color coordinates of the WOLEDs at 5% and 10% Firpic doping concentrations were (0.49, 0.41) and (0.45, 0.41), which corresponded to warm white color.

To further manage the emission spectra of the WOLEDs, the thickness of the red emitting layer was reduced to 1 nm. The thickness of the blue/green emitting layer was 24 nm. The EL spectra with the thin red emitting layer is presented in Figure 5. The blue/green intensity was increased by optimizing the thickness of blue/green and red emitting layers, resulted in warm white color coordinate of (0.43, 0.42) at 1,000 cd/m². Comparing the EL spectra of the hybrid WOLEDs with 1 nm thick red emitting layer at different luminances, there was little change of the EL spectra from 10 cd/m² to 1,000 cd/m². The color coordinates of the hybrid WOLED at 10, 100, 1,000 cd/m² were (0.45, 0.43), (0.44, 0.42) and (0.43, 0.42). There was less than 0.02 shift of the x and y coordinates of the WOLEDs. The relative light emission intensity of the blue/green to red was maintained constant and the light emission intensity of Firpic compared to green emitting 4CzIPN was also kept stable.

Discussion

The hybrid OLEDs doped with Firpic and 4CzIPN showed high quantum efficiency possibly due to efficient energy transfer from

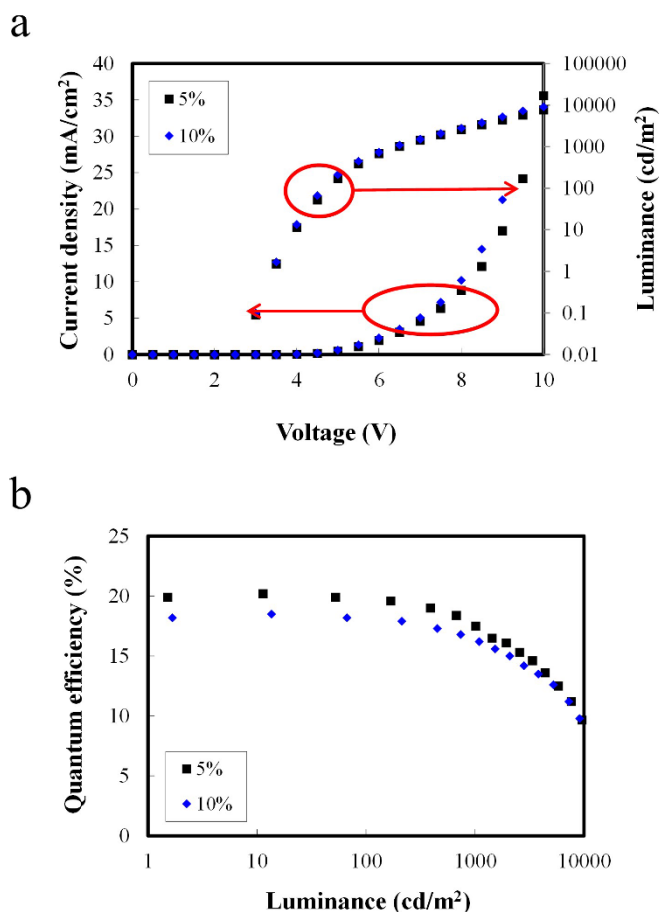


Figure 3 | Current density-voltage-luminance curves (a) and quantum efficiency-luminance curves (b) of hybrid WOLEDs with different Firpic doping concentrations.

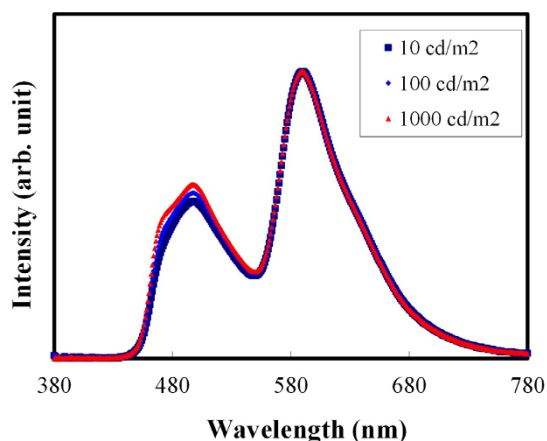


Figure 5 | EL spectra of WOLEDs with 24 nm thick mCP:Firpic:4CzIPN emitting layer and 1 nm thick TPBI:Ir(pq)₂acac emitting layer at different luminances.



Flrpic to 4CzIPN without non-radiative triplet exciton quenching of Flrpic by 4CzIPN. In order to study the energy transfer between phosphorescent emitters and a TADF emitter, photoluminescence (PL) measurement of mCP, mCP:Flrpic, mCP:4CzIPN and mCP:Flrpic:4CzIPN was carried out. Doping concentration of Flrpic was 5% in all films. Doping concentration of 4CzIPN in the mCP:4CzIPN film was 3% and the doping concentrations of 4CzIPN in the mCP:Flrpic:4CzIPN were 1% and 3%. Figure 6(a) shows PL spectra of the vacuum deposited films. Energy transfer efficiency was calculated from the PL intensity of mCP in the organic films by exciting the film using 310 nm light source. The energy transfer efficiencies from mCP to Flrpic and mCP to 4CzIPN were 0.96 and 0.85. The energy transfer from mCP to dopant materials was more efficient in the mCP:Flrpic film than in the mCP:4CzIPN film. The energy transfer efficiency was further improved by co-doping Flrpic and 4CzIPN in the mCP host and it was 0.97 in the mCP:Flrpic:4CzIPN film at 1% and 3% 4CzIPN doping concentrations. This indicates that the energy transfer from mCP to dopant materials in the Flrpic and 4CzIPN co-doped emitting layer is very efficient.

The energy transfer from Flrpic to 4CzIPN was further characterized by exciting Flrpic of mCP:Flrpic:4CzIPN using 370 nm light source. There is no absorption of the mCP host material at 370 nm and the excitation using this light source can excite only Flrpic and 4CzIPN without any excitation of mCP. PL spectra of mCP:Flrpic:4CzIPN film excited using 370 nm light source are presented in Figure 6(b). The intensity of Flrpic in the mCP:Flrpic and mCP:Flrpic:4CzIPN films was compared. Doping concentration of Flrpic was 5% and the doping concentrations of 4CzIPN were 1% and 3%. The Flrpic emission is clearly observed at 1% 4CzIPN doping concentration, but it almost disappeared at 3% 4CzIPN doping concentration, suggesting efficient energy transfer from Flrpic to 4CzIPN at 3% doping concentration.

As the Flrpic triplet emitter and 4CzIPN TADF emitter were doped in the mCP at the same time, delayed PL emission of the mCP:Flrpic:4CzIPN hybrid film was investigated by time resolved PL measurement. Delayed PL spectrum of mCP:Flrpic:4CzIPN with 5% Flrpic and 1% 4CzIPN is shown in Figure 6(c). Delay time for the measurement was 1 μ s. Main emission peak was observed at 498 nm due to delayed fluorescence of 4CzIPN and a weak shoulder was detected at 470 nm by phosphorescent emission of Flrpic. As the excited state lifetime of Flrpic (1.2 μ s)²⁸ is shorter than that of 4CzIPN (5.1 μ s)¹⁶, the light emission after 1 μ s was dominated by 4CzIPN emission. Compared with the prompt PL emission spectrum of mCP:Flrpic:4CzIPN, the 4CzIPN emission was intensified due to delayed emission by reverse intersystem crossing from triplet excited state to singlet excited state. It can be inferred from this result that the Flrpic activates the delayed emission of 4CzIPN through efficient energy transfer, which resulted in the high quantum efficiency of the hybrid OLEDs.

As the delayed fluorescence of 4CzIPN was activated and the radiative energy transfer from Flrpic to 4CzIPN was efficient, it was possible to develop high efficiency hybrid WOLEDs using the 4CzIPN delayed fluorescent material. High quantum efficiency above 20% was observed and the high quantum efficiency of the hybrid WOLEDs is related with the high quantum efficiency of the mCP:Flrpic:4CzIPN hybrid OLEDs. As the 4CzIPN dopant did not non-radiatively quench triplet emission of Flrpic, high quantum efficiency could be obtained in the hybrid WOLEDs with a TADF dopant. In the case of common fluorescent green dopant, the fluorescent green dopant quenches triplet emission of phosphorescent dopant and reduces quantum efficiency of the WOLEDs. The suppression of triplet exciton quenching and energy transfer from Flrpic to 4CzIPN improved the quantum efficiency of the hybrid WOLEDs. In addition, balanced charge density in the emitting layer also contributed to the high quantum efficiency of the hybrid WOLEDs. The TPBI:Ir(pq)₂acac emitting layer efficiently injects electrons due to

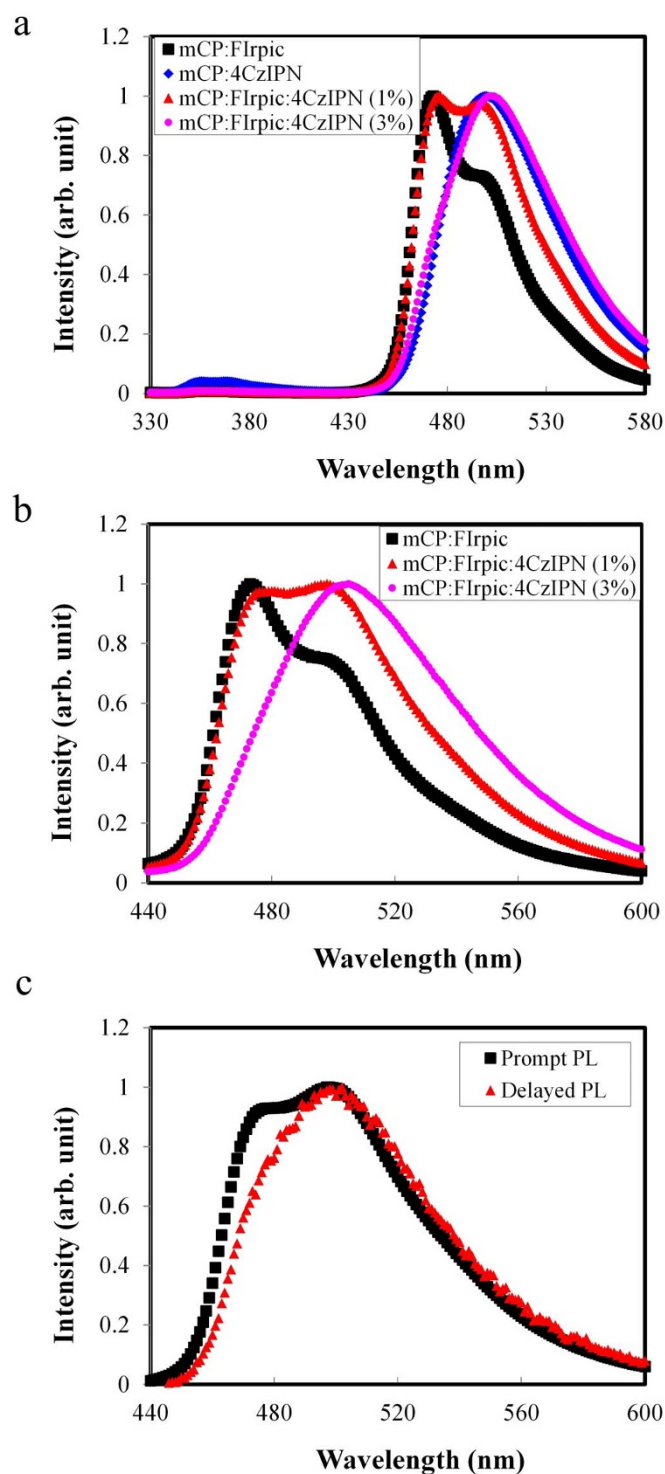


Figure 6 | PL spectra of mCP:Flrpic, mCP:4CzIPN and mCP:Flrpic:4CzIPN films excited by 310 nm light source (a) and PL spectra of mCP:Flrpic, and mCP:Flrpic:4CzIPN films excited by 370 nm light source (b). Doping concentrations of 4CzIPN in the mCP:Flrpic:4CzIPN films were 1% and 3%. Doping concentration of Flrpic was 5% in all films and the doping concentration of 4CzIPN in the mCP:4CzIPN film was 3%. Prompt and delayed PL spectra of mCP:Flrpic:4CzIPN film with a delay time of 1 μ s (c). Doping concentration of 4CzIPN in the mCP:Flrpic:4CzIPN films was 1%.

electron transport properties of TPBI, which improved charge balance in the emitting layer in combination with hole transport type mCP:Flrpic:4CzIPN emitting layer. Therefore, this approach to

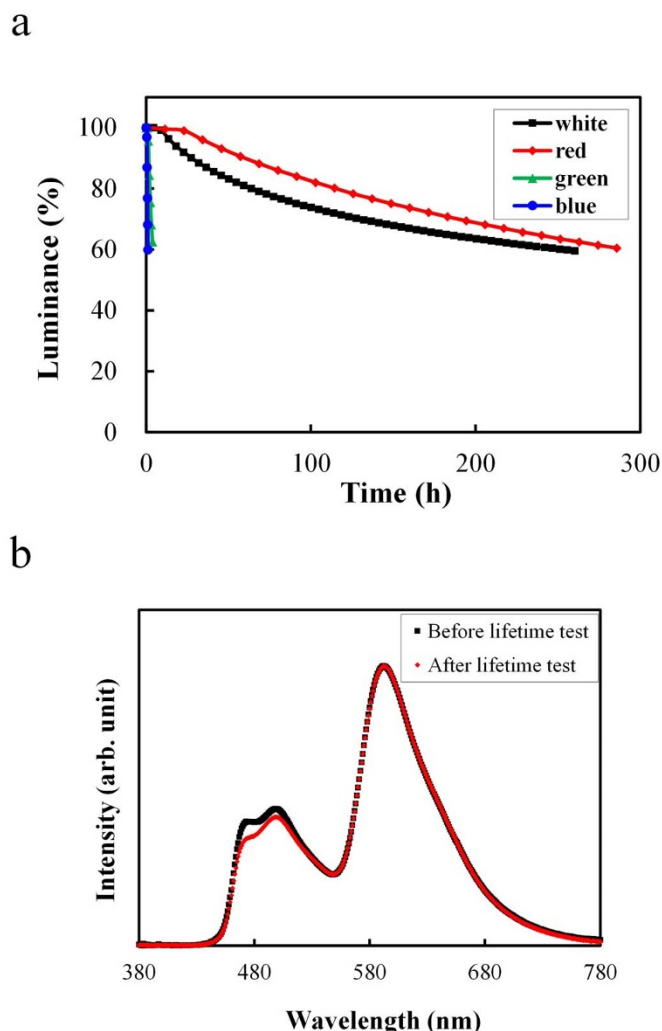


Figure 7 | Lifetime of the red, green, blue and white devices measured at an initial luminance of 100 cd/m² in a constant current mode (a). Device structure of red, green and blue devices was ITO (50 nm)/PEDOT:PSS (60 nm)/TAPC (20 nm)/mCP (10 nm)/host:dopant (25 nm)/TSPO1 (35 nm)/LiF (1 nm)/Al (200 nm). Host:dopant systems for red, green and blue devices were TPBI:Ir(pq)₂acac, mCP:4CzIPN and mCP:FIrpic. EL spectra of the white device before and lifetime test up to 60% of initial luminance (b).

adopt TADF green emitting material in the hybrid WOLED is effective to enhance the quantum efficiency of the hybrid WOLEDs.

Lifetime of the hybrid WOLEDs was compared with the lifetime of single color devices. Figure 7 (a) shows the lifetime curves of white and single color OLEDs at a constant current mode with an initial luminance of 100 cd/m². The lifetime of the white device up to 60% of initial luminance was similar to that of the red device. Although the lifetime of the green and blue devices was very short, the lifetime of the white device was comparable to that of the red device because of rather strong red emission of the white device. Normalized EL spectra of the white devices before and after lifetime test is shown in Figure 7 (b). Relative decrease of the blue intensity was observed due to poor stability of the blue triplet emitter.

In conclusion, hybrid WOLEDs with a green TADF emitter and blue/red phosphorescent emitters were developed by stacking the red emitting layer on hybrid emitting layer of blue triplet emitter and green TADF emitter. The triplet emission of blue emitting FIrpic dopant was transferred to 4CzIPN dopant with little quenching, which resulted in high quantum efficiency of 19.2% in hybrid OLEDs of mCP:FIrpic:4CzIPN and 20.2% in the hybrid WOLEDs.

The quantum efficiency of the hybrid WOLEDs was comparable to that of all phosphorescent WOLEDs and further development of the device structure and emitting materials may enhance the quantum efficiency of the hybrid WOLEDs.

Methods

Device fabrication. Device structure of the hybrid OLEDs of FIrpic and 4CzIPN was ITO (50 nm)/PEDOT:PSS (60 nm)/TAPC (20 nm)/mCP (10 nm)/mCP:FIrpic:4CzIPN (25 nm)/TSPO1 (35 nm)/LiF (1 nm)/Al (200 nm). The doping concentration of FIrpic was 5% and the doping concentrations of 4CzIPN were 0.5, 1 and 3%. Hybrid WOLEDs had a standard device structure of ITO (50 nm)/PEDOT:PSS (60 nm)/TAPC (20 nm)/mCP (10 nm)/mCP:FIrpic:4CzIPN (12.5 nm)/TPBI:Ir(pq)₂acac (12.5 nm, 3%)/TSPO1 (35 nm)/LiF (1 nm)/Al (200 nm). The doping concentrations of FIrpic were 5 and 10%, and that of 4CzIPN was fixed at 1 wt%. In addition, hybrid WOLED with 24 nm thick mCP:FIrpic:4CzIPN and 1 nm thick TPBI:Ir(pq)₂acac (12.5 nm, 3%) was also fabricated. PEDOT:PSS layer was spin coated on the ITO substrate and other materials were deposited by vacuum thermal evaporation. Devices were encapsulated using a glass cover after device fabrication inside a glove box.

Measurements. Solid PL spectra of the mCP:FIrpic, mCP:4CzIPN and mCP:FIrpic:4CzIPN films were obtained using fluorescence spectrophotometer (HITACHI, F-7000). Excitation wavelengths were 310 nm and 370 nm. Current density-voltage curves were recorded using Keithley 2400 source measurement unit and luminance-voltage curves were obtained using the Keithley 2400 source measurement unit and CS1000 spectroradiometer. External quantum efficiency was calculated from the current density and luminance of the devices based on Lambertian distribution of light emission. All device performances were measured in ambient condition after encapsulation of the fabricated device.

- Reineke, S. *et al.* White organic light-emitting diodes with fluorescent tube efficiency. *Nature* **459**, 234–238 (2009).
- Sun, Y. R. *et al.* Management of singlet and triplet excitons for efficient white organic light-emitting devices. *Nature* **440**, 908–912 (2006).
- Kido, J., Kimura, M. & Nagai, K. Multilayer white light-emitting organic electroluminescent device. *Science* **267**, 1332–1334 (1995).
- Su, S.-J., Gomori, E., Sasabe, H. & Kido, J. Highly efficient organic blue and white light-emitting devices having a carrier and exciton confining structure for reduced efficiency roll-off. *Adv. Mater.* **20**, 4189–4194 (2008).
- Sun, Y. & Forrest, S. R. High-efficiency white organic light emitting devices with three separate phosphorescent emission layers. *Appl. Phys. Lett.* **91**, 263503 (2007).
- Schwartz, G. *et al.* Highly efficient white organic light emitting diodes comprising an interlayer to separate fluorescent and phosphorescent regions. *Appl. Phys. Lett.* **89**, 083509 (2006).
- Eom, S.-H. *et al.* White phosphorescent organic light-emitting devices with dual triple-doped emissive layers. *Appl. Phys. Lett.* **94**, 153303 (2009).
- Ho, C.-L. *et al.* High-efficiency and color-stable white organic light-emitting devices based on sky blue electrofluorescence and orange electrophosphorescence. *Appl. Phys. Lett.* **92**, 083301 (2008).
- Han, C. *et al.* A Single Phosphine Oxide Host for High-Efficiency White Organic Light-Emitting Diodes with Extremely Low Operating Voltages and Reduced Efficiency Roll-Off. *Adv. Mater.* **23**, 2491–2495 (2011).
- Seo, C. W. & Lee, J. Y. High efficiency in two color and three color phosphorescent white organic light-emitting diodes using a 2,7-substituted 9-phenylcarbazole derivative as the host material. *Org. Electron.* **12**, 1459–1464 (2011).
- Wang, Q. *et al.* Highly efficient single-emitting-layer white organic light-emitting diodes with reduced efficiency roll-off. *Appl. Phys. Lett.* **94**, 103503 (2009).
- Schwartz, G. *et al.* Triplet Harvesting in Hybrid White Organic Light-Emitting Diodes. *Adv. Funct. Mater.* **19**, 1319–1333 (2009).
- Schwartz, G. *et al.* Harvesting Triplet Excitons from Fluorescent Blue Emitters in White Organic Light-Emitting Diodes. *Adv. Mater.* **19**, 3672–3676 (2007).
- Kondakova, M. E. *et al.* Highly efficient fluorescent-phosphorescent triplet-harvesting hybrid organic light-emitting diodes. *J. Appl. Phys.* **107**, 014515 (2010).
- Zheng, C. *et al.* Novel Efficient Blue Fluorophors with Small Singlet-Triplet Splitting: Hosts for Highly Efficient Fluorescence and Phosphorescence Hybrid WOLEDs with Simplified Structure. *Adv. Mater.* **25**, 2205–2211 (2013).
- Uoyama, H. *et al.* Highly efficient organic light-emitting diodes from delayed fluorescence. *Nature* **492**, 236–240 (2012).
- Dias, F. B. *et al.* Triplet Harvesting with 100% Efficiency by Way of Thermally Activated Delayed Fluorescence in Charge Transfer OLED Emitters. *Adv. Mater.* **25**, 3707–3714 (2013).
- Goushi, K., Yoshida, K., Sato, K. & Adachi, C. Organic light-emitting diodes employing efficient reverse intersystem crossing for triplet-to-singlet state conversion. *Nat. Photonics* **6**, 253–258 (2012).
- Zhang, Q. *et al.* Design of Efficient Thermally Activated Delayed Fluorescence Materials for Pure Blue Organic Light Emitting Diodes. *J. Am. Chem. Soc.* **134**, 14706–14709 (2012).



20. Li, J. *et al.* Highly Efficient Organic Light-Emitting Diode Based on a Hidden Thermally Activated Delayed Fluorescence Channel in a Heptazine Derivative. *Adv. Mater.* **25**, 3319–3323 (2013).
21. Lee, S. Y., Yasuda, T., Nomura, H. & Adachi, C. High-efficiency organic light-emitting diodes utilizing thermally activated delayed fluorescence from triazine-based donor–acceptor hybrid molecules. *Appl. Phys. Lett.* **101**, 093306 (2012).
22. Nakagawa, T., Ku, S.-Y., Wong, K.-T. & Adachi, C. Electroluminescence based on thermally activated delayed fluorescence generated by a spirobifluorene donor–acceptor structure. *Chem. Commun.* **48**, 9580–9582 (2012).
23. Tanaka, H., Shizu, K., Miyazaki, H. & Adachi, C. Efficient green thermally activated delayed fluorescence (TADF) from a phenoxazine–triphenyltriazine (PXZ–TRZ) derivative. *Chem. Commun.* **48**, 11392–11394 (2012).
24. Czerwieniec, R., Kowalski, K. & Yersin, H. Highly efficient thermally activated fluorescence of a new rigid Cu(I) complex [Cu(dmp)(phanephos)]⁺. *Dalton Trans.* **42**, 9826–9830 (2013).
25. Yersin, H. *et al.* The triplet state of organo-transition metal compounds. Triplet harvesting and singlet harvesting for efficient OLEDs. *Coord. Chem. Rev.* **255**, 2622–2652 (2011).
26. Czerwieniec, R., Yu, J. & Yersin, H. Blue-Light Emission of Cu(I) Complexes and Singlet Harvesting. *Inorg. Chem.* **50**, 8293–8301 (2011).
27. Zink, D. M. *et al.* Synthesis, Structure, and Characterization of Dinuclear Copper(I) Halide Complexes with P[^]N Ligands Featuring Exciting Photoluminescence Properties. *Inorg. Chem.* **52**, 2292–2305 (2013).
28. Son, H. S., Seo, C. W. & Lee, J. Y. Correlation of the substitution position of diphenylphosphine oxide on phenylcarbazole and device performances of blue phosphorescent organic light-emitting diodes. *J. Mater. Chem.* **21**, 5638–5644 (2011).

Acknowledgments

This research was supported by Basic Science Research Program through the National Research Foundation of Korea(NRF) funded by the Ministry of Education, Science and Technology(2013R1A1A2007991) and Ministry of Science, ICT and future Planning (2013R1A2A2A010674).

Author contributions

B.K. fabricated the hybrid organic light-emitting diodes and hybrid white organic light-emitting diodes and measured device performances. K.Y. analyzed the device data of the hybrid devices and designed the device structure of the hybrid devices. J.L. supervised all experiments and prepared the manuscript for submission. All authors reviewed the manuscript and contributed to this work

Additional information

Competing financial interests: The authors declare no competing financial interests.

How to cite this article: Kim, B.S., Yook, K.S. & Lee, J.Y. Above 20% external quantum efficiency in novel hybrid white organic light-emitting diodes having green thermally activated delayed fluorescent emitter. *Sci. Rep.* **4**, 6019; DOI:10.1038/srep06019 (2014).



This work is licensed under a Creative Commons Attribution-NonCommercial-NoDerivs 4.0 International License. The images or other third party material in this article are included in the article's Creative Commons license, unless indicated otherwise in the credit line; if the material is not included under the Creative Commons license, users will need to obtain permission from the license holder in order to reproduce the material. To view a copy of this license, visit <http://creativecommons.org/licenses/by-nc-nd/4.0/>